IEEE Access
Multidisciplinary | Rapid Review | Open Access Journal

Received June 23, 2019, accepted July 14, 2019, date of publication July 16, 2019, date of current version August 2, 2019.

Digital Object Identifier 10.1109/ACCESS.2019.2929305

Joint Compressed Sensing and Enhanced Whale Optimization Algorithm for Pilot Allocation in Underwater Acoustic OFDM Systems

RONGKUN JIANG[1], XUETIAN WANG[1], SHAN CAO[2], JIAFEI ZHAO[1], AND XIAORAN LI[1]
[1]School of Information and Electronics, Beijing Institute of Technology, Beijing 100081, China
[2]Department of Communication and Information Engineering, Shanghai University, Shanghai 200444, China

Corresponding author: Xiaoran Li (xiaoran.li@bit.edu.cn)

This work was supported in part by the National Natural Science Foundation of China under Grant 61801024 and Grant 61801027, and in part by the China Postdoctoral Science Foundation under Grant 2018M631356.

ABSTRACT In underwater acoustic-orthogonal frequency division multiplexing (UWA-OFDM) systems, the performance of channel estimation is significantly affected by pilot allocation in the framework of compressed sensing (CS). However, for optimizing the pilot allocation, an exhaustive search method over all possible allocations is computationally prohibitive and random search method may not ensure convergence accuracy. In this paper, the meta-heuristic algorithm of the whale optimization algorithm (WOA) is employed to address this issue. For reinforcing the capability of balancing exploration and exploitation, an enhanced variant of WOA termed EWOA is presented with four optimization strategies. After that, a joint algorithm combining CS with EWOA (CS-EWOA) is proposed for pilot allocation in UWA-OFDM systems. Through extensive simulations, the improvement of EWOA is demonstrated on the majority of benchmark functions over other well-known meta-heuristic algorithms. With regard to bit error rate (BER) and mean square error (MSE) for channel estimation, the proposed CS-EWOA algorithm outperforms the equispaced, random, genetic algorithm (GA), particle swarm optimization (PSO), and WOA-based pilot allocation methods. Moreover, it is robust with varying system subcarriers and channel models. Furthermore, the CS-EWOA exhibits superior convergence performance without increasing the computational complexity compared with the GA-, PSO-, and WOA-based methods in the iteration process of pilot allocation optimization. It can be concluded from the simulation results that the proposed CS-EWOA algorithm is competitive to optimize pilot allocation for channel estimation in UWA-OFDM systems.

INDEX TERMS Compressed sensing, OFDM, whale optimization algorithm, underwater acoustic communication, channel estimation, pilot allocation.

I. INTRODUCTION

In recent years, orthogonal frequency division multiplexing (OFDM) has been drawing attention in the field of underwater acoustic (UWA) communication, which is usually regarded as one of the most complicated communication mediums [1]–[3]. By transforming the channel bandwidth into parallel orthogonal narrowband subcarriers, OFDM technique can effectively alleviate the various channel distortions and interferences, such as multipath fading effect, Doppler frequency shift, and inter symbol interference (ISI). The special modulation mechanism ensures the OFDM system with high-speed transmission and high spectrum efficiency over UWA multipath channels.

For UWA-OFDM systems, the communication quality often depends on the performance of channel estimation, in which the channel state information (CSI) can be attained. Since the transmitted signal is generally distorted when passing through the UWA channel, CSI is indispensable for data detection and demodulation at the receiver. In channel estimation, the most common methods to obtain CSI are assisted by pilot symbols. Except for least square (LS) and minimum mean square error (MMSE) [4], compressed sensing (CS) [5] has also been adopted to handle the channel estimation problem in OFDM systems recently [6]–[10]. Since the UWA multipath channel is usually considered as sparse, CS is

The associate editor coordinating the review of this manuscript and approving it for publication was Chenhao Qi.

especially applicable to solve such reconstruction problem by exploiting the inherent sparsity in the channel impulse response (CIR) of UWA channel. Through extensive investigation, CS has demonstrated its advantages in both ameliorating estimation accuracy and reducing system overhead than the conventional LS and MMSE methods.

In CS-based channel estimation, the main challenge is to optimize the pilot allocation, which is usually determined by constructing a suitable measurement matrix to satisfy the restricted isometry property (RIP) condition [5] for improving the reconstruction probability of CSI. Reference [11] revealed that the smaller the mutual coherence is, the more the measurement matrix matches RIP. In theory, the optimal measurement matrix can be selected by exhausting all the possible pilot allocations. Nonetheless, it is impracticable in real UWA-OFDM systems due to the huge amount of computation caused by the large number of system subcarriers and pilot symbols. Therefore, it is necessary to search the optimal pilot allocation as accurately and quickly as possible. To tackle this problem, [12] focused on a random search method within the specified subsets by minimizing the mutual coherence of the measurement matrix. In [13]–[15], the methods of cross-entropy optimization, modified discrete stochastic approximation and its variants were used to optimize the pilot placement. However, the aforementioned methods may suffer from difficulties in convergence time and convergence accuracy when searching the optimal pilot allocation.

A. RELATED WORK

In the past few decades, meta-heuristic algorithms have become increasingly popular in many optimization problems with the advantages of rather simple concept, easy implementation, and no need for gradient information. They are essentially regarded as iterative systems, in which the goal of global optimization can be achieved by initializing the population, calculating the fitness of each individual, generating new individuals, updating the population in each iteration, and selecting the best individual through appropriate strategies. The typical representatives of these algorithms include genetic algorithm (GA) [16], particle swarm optimization (PSO) [17], artificial bee colony (ABC) [18], bat-inspired algorithm (BA) [19], grey wolf optimizer (GWO) [20], and more recent whale optimization algorithm (WOA) [21]. With the development of meta-heuristic algorithms, they have been applied in wide ranges of complex optimization problems and engineering applications [22]–[24].

It is noteworthy that pilot allocation for channel estimation in UWA-OFDM systems is also a combinatorial optimization problem. Naturally, many meta-heuristic algorithms have been attracted great research interests to deal with such issue. In [25]–[28], the GA and PSO algorithms were adopted to optimize pilot allocation for channel estimation in OFDM systems, as well as ABC [29], GWO [30], and firefly algorithm (FA) [31]. Moreover, a few hybrid techniques with various basic algorithms have been proposed to obtain better performance, such as cooperative PSO (CPSO) [32], modified adaptive GA (MAGA) [33], PSO-GA [34], and GWO-GA [35]. However, almost all these studies are based on LS algorithm by minimizing the estimation error of mean square error (MSE) criterion. Inevitably, these algorithms do not make full use of the significant sparsity of UWA multipath channels to improve the spectral efficiency of the communication system. In this paper, we attempt to solve the pilot allocation optimization problem more efficiently by virtue of the advantages of CS theory and meta-heuristic algorithms.

WOA is a novel meta-heuristic optimization algorithm proposed in 2016 [21]. This algorithm takes inspiration from the foraging behavior of humpback whales, called bubble-net feeding method [36]. Compared with other popular meta-heuristic algorithms such as GA and PSO, the WOA algorithm is simple in concepts but powerful to explore global solutions. Currently, some variants of the WOA algorithm have emerged in literatures to further improve the performance, since WOA is also not perfect. The competitive performance of WOA and its variants have been successfully demonstrated to the solution of complex optimization problems. In [37] and [38], WOA was optimized to accurately extract the parameters of solar cells and photovoltaic modules. In [39], chaotic whale optimization algorithm (CWOA) was demonstrated to be well capable for the transient stability constrained optimal power flow problem of power system. Reference [40] adopted the CWOA to optimize the Elman neural network soft-sensor model of conversion velocity in polymerization process. Reference [41] improved the WOA based on a Lévy flight trajectory, resulting faster and more robust convergence. Furthermore, a hybrid algorithm was combined WOA with maximum person maximum distance algorithm for feature selection and classification in [42]. In [43], a hybrid WOA was proposed with the aid of modified differential evolution (DE) for global optimization problems. Similarly, [44] combined WOA with PSO for image segmentation. However, these variants of the WOA algorithm are usually optimized only for one or two aspects, slightly lacking in comprehensive and systematic consideration.

B. OUR CONTRIBUTION

As stated previously, although WOA and its variants have already been applied to various fields, there is no study related to the optimization problem of pilot allocation for channel estimation in UWA-OFDM systems. Therefore, we are devoted to employing the essence of WOA to bear on the pilot allocation problem. At first, in this work, an enhanced WOA algorithm (EWOA) is improved with four different strategies to accomplish a better tradeoff between the exploration and exploitation of the algorithm. A joint CS and EWOA algorithm termed as CS-EWOA is then proposed to chase the optimal pilot allocation for channel estimation. Through numerical simulations, the proposed EWOA algorithm is tested on solving benchmark functions and compared with representative meta-heuristic optimization algorithms mathematically. Moreover, the channel estimation performance of

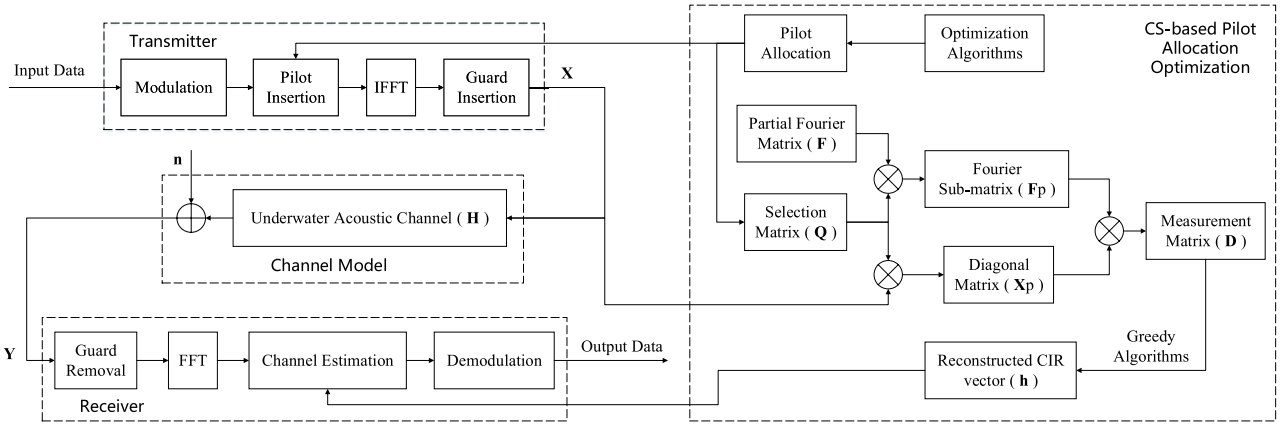

FIGURE 1. Simplified block diagram of UWA-OFDM system model including three parts of transmitter, receiver, and channel model. To improve the system performance, assisted pilot symbols are inserted at the transmitter via CS-based pilot allocation optimization algorithms and then utilized for channel estimation at the receiver to evaluate the characteristics of channel model.

the joint CS-EWOA pilot allocation algorithm is evaluated in terms of BER and MSE, convergence speed, and computational complexity.

The primary contribution of our work can be summarized as follows:

1) We ameliorate a novel variant of the WOA algorithm as EWOA to further improve the performance through four optimization strategies, which differ from the existing research as here they have been tailored to suit the application framework of the algorithm.
2) We propose a joint CS-EWOA algorithm, combining the advantages of both, to address the pilot allocation optimization for channel estimation in UWA-OFDM systems.
3) We perform extensive simulations to validate the improvement of EWOA over classical benchmark functions and compare the channel estimation performance of CS-EWOA with the equispaced, random, GA, PSO, and standard WOA based pilot allocation methods in different conditions.

According to the statistic results on benchmark functions, the EWOA algorithm is verified with a better optimization capability than other considered meta-heuristic algorithms. For channel estimation performance, the robustness and effectiveness of the proposed CS-EWOA algorithm are demonstrated by maintaining consistent performance superiority with respect to BER and MSE for different system subcarriers and channel models. Additionally, simulation results confirm that our proposal retains almost the same computational complexity but yields better convergence performance than the GA, PSO, and WOA based methods in optimizing pilot allocations.

The remaining portion of this paper is organized as follows. In Section II, the UWA-OFDM system model and CS-based channel estimation problem are described briefly. In Section III, the standard WOA, the ameliorative EWOA, the proposed CS-EWOA algorithm and its application in pilot allocation for channel estimation are presented in detail. In Section IV, simulations and results of the considered methods are given and analyzed. Finally, Section V is devoted to conclusions.

II. PROBLEM FORMULATION

A. CHANNEL ESTIMATION IN UWA-OFDM SYSTEMS

A simplified block diagram of the UWA-OFDM system [45] for wireless communication is shown in Fig. 1.

UWA multipath channels are usually sparse by exhibiting that only a small number of channel taps are non-zero whereas most of them are either zero or nearly zero. It means that the channel impulse response (CIR) will be contributed with these significant non-zero taps [7], [8]. Therefore, a time-varying UWA channel, whose coherence time is much larger than the period of an OFDM symbol, can be modeled as [46], [47]:

$$h(t,\tau) = \sum_{i=1}^{L} \alpha_i \delta(\tau - (\tau_i - \varepsilon_i \cdot t)) \tag{1}$$

where L is the total number of paths, α_i and τ_i refer to the real amplitude and time delay of the i-th path. In this model, the path amplitude and delay are supposed slowly changing over the duration of an OFDM symbol. According to [7], [8], [48]–[50], the Doppler spread in underwater environment can be reasonably characterized as a non-uniform model with dynamic Doppler scaling factors ε_i for different paths.

Consider a UWA-OFDM system consists of N subcarriers, and $P(P \leq N)$ subcarriers out of them are allocated as pilot symbols to assist for channel estimation. It is assumed that the set of pilot positions is $\Lambda = \{\Lambda_1, \Lambda_2, \ldots, \Lambda_P\}(1 \leq \Lambda_1 < \ldots < \Lambda_P \leq N)$. At the transmitter, pilot symbols are usually embedded in data symbols before transmission. With the operation of inverse fast Fourier transform (IFFT), assume the transmitted signal, including the modulated data and pilot symbols, is represented as $x_i(i = 1, 2, \ldots, N)$ in time domain. Through the UWA multipath channel, the received

signal in time domain $y_i(i = 1, 2, \ldots, N)$ can be obtained at the receiver. Then, after fast Fourier transform (FFT), the frequency domain signal of y_i is denoted as:

$$\mathbf{Y} = \mathbf{XH} + \mathbf{n} = \mathbf{XFh} + \mathbf{n} \tag{2}$$

where $\mathbf{X} = diag(x_1, x_2, \ldots, x_N)$ is a $N \times N$ diagonal matrix containing the transmitted signal, $\mathbf{h} = [h(1), h(2), \ldots, h(L)]^T$ is an $L \times 1$ CIR vector of the K-sparse ($K \ll N$) channel, $\mathbf{H} = \mathbf{Fh}$ is the $N \times 1$ channel frequency response (CFR) vector, and $\mathbf{n}$ is the $N \times 1$ additive white Gaussian noise (AWGN) vector. Besides, $\mathbf{F}$ stands for the $N \times L$ partial Fourier matrix, which consists of only the first L columns from the $N \times N$ standard Fourier transform matrix, given by:

$$\mathbf{F} = \frac{1}{\sqrt{N}} \begin{bmatrix} f_{1,1} & f_{1,2} & \cdots & f_{1,L} \\ f_{2,1} & f_{2,2} & \cdots & f_{2,L} \\ \vdots & \vdots & \ddots & \vdots \\ f_{N,1} & f_{N,2} & \cdots & f_{N,L} \end{bmatrix} \tag{3}$$

where $f = e^{-j2\pi/N}$.

Defining a $P \times N$ selection matrix $\mathbf{Q}$ is generated by the positions of P pilot symbols corresponding to the rows of the identity matrix. Thus, the transmitted pilot symbols are:

$$\mathbf{X}_p = \mathbf{QXQ}^T \tag{4}$$

where $\mathbf{X}_p$ is a $P \times P$ diagonal matrix. Similarly, based on (2), the received pilot symbols are given by:

$$\mathbf{Y}_p = \mathbf{QY} = \mathbf{X}_p\mathbf{F}_p\mathbf{h} + \mathbf{n}_p \tag{5}$$

where $\mathbf{n}_p = \mathbf{Qn}$ is a $P \times 1$ noise vector, and $\mathbf{F}_p$ is a $P \times L$ Fourier sub-matrix constituted by the P pilot indexes, defined as:

$$\mathbf{F}_p = \mathbf{QF} \tag{6}$$

Let the $P \times L$ sized measurement matrix be:

$$\begin{aligned} \mathbf{D} &= \mathbf{X}_p\mathbf{F}_p \\ &= \frac{1}{\sqrt{N}} \begin{bmatrix} x_{\Lambda_1} f_{\Lambda_1,1} & x_{\Lambda_1} f_{\Lambda_1,2} & \cdots & x_{\Lambda_1} f_{\Lambda_1,L} \\ x_{\Lambda_2} f_{\Lambda_2,1} & x_{\Lambda_2} f_{\Lambda_2,2} & \cdots & x_{\Lambda_2} f_{\Lambda_2,L} \\ \vdots & \vdots & \ddots & \vdots \\ x_{\Lambda_p} f_{\Lambda_p,1} & x_{\Lambda_p} f_{\Lambda_p,2} & \cdots & x_{\Lambda_p} f_{\Lambda_p,L} \end{bmatrix} \end{aligned} \tag{7}$$

so (5) can be rewritten as:

$$\mathbf{Y}_p = \mathbf{Dh} + \mathbf{n}_p \tag{8}$$

It is clearly from (8) that the received pilot symbols $\mathbf{Y}_p$ and the measurement matrix $\mathbf{D}$ are known to the receiver for channel estimation. Specifically, if a suitable measurement matrix could be designed, the sparse CIR vector $\mathbf{h}$ can be evaluated accurately in noisy environment by exploiting CS-based greedy reconstruction algorithms, such as orthogonal matching pursuit (OMP) [51], compressive sampling matching pursuit (CoSaMP) [52], etc. Therefore, the channel estimation problem in UWA-OFDM systems can be transformed to design the measurement matrix in the framework of CS theory.

B. CS-BASED PILOT ALLOCATION OPTIMIZATION

According to the CS theory, the measurement matrix $\mathbf{D}$ is required to obey the RIP condition to ensure a high probability of reconstructing the sparse vector $\mathbf{h}$ [53]. However, it is difficult to calculate and check whether a measurement matrix satisfies the RIP condition because of the high computational complexity involved. A widely used alternative condition, called the mutual coherence of the measurement matrix, was proposed for reducing the computational complexity [54]–[56]. More intuitive and practical than RIP, this criterion is defined as the largest absolute inner product between two different normalized columns of the measurement matrix $\mathbf{D}$ [57], as follows:

$$\mu(\mathbf{D}) = \max_{1 \le m,n \le L, m \ne n} \left\{ \frac{\left| \langle \mathbf{d}_m^H \mathbf{d}_n \rangle \right|}{\|\mathbf{d}_m\|_2 \cdot \|\mathbf{d}_n\|_2} \right\} \tag{9}$$

where $\mathbf{d}_m$ and $\mathbf{d}_n$ are the normalized column vectors of $\mathbf{D}$, superscript H refers to the complex conjugate transpose, and $\|\cdot\|_2$ denotes the 2-norm. If (7) is substituted to (9), it can be obtained:

$$\mu(\mathbf{D}) = \max_{1 \le m,n \le L, m \ne n} \frac{\left| \sum_{i=1}^{P} |x_{\Lambda_i}|^2 e^{-j2\pi(n-m)\Lambda_i/N} \right|}{\sum_{i=1}^{P} |x_{\Lambda_i}|^2} \tag{10}$$

Clearly, (10) reveals that the mutual coherence of measurement matrix $\mathbf{D}$ is determined by pilot symbol values and pilot allocation positions simultaneously. In this paper, we only focus on the effect of pilot allocation positions for CS-based channel estimation so that all the values of pilot symbols are assumed to $|x_{\Lambda_i}| = 1 (i = 1, 2, \ldots, P)$ to simplify the optimization problem. Then (10) can be rewritten as:

$$\mu(\mathbf{D}) = \max_{1 \le m,n \le L, m \ne n} \frac{1}{P} \left| \sum_{i=1}^{P} e^{-j2\pi(n-m)\Lambda_i/N} \right| \tag{11}$$

Since minimizing the mutual coherence of measurement matrix has been proven an effective approach to improve the reconstruction performance [7], it is feasible to design a measurement matrix with mutual coherence as small as possible. Under the assumption of ignoring the effect of pilot symbol values, now the core of this optimization problem is how to select P subcarriers as pilot symbols from N subcarriers in UWA-OFDM systems to achieve the minimal mutual coherence. Therefore, the problem of pilot allocation optimization can be defined as:

$$\begin{aligned} \Lambda_{opt} &= \arg\min_{\Lambda} \{\mu(\mathbf{D})\}, \\ s.t. \Lambda &= \{\Lambda_1, \Lambda_2, \ldots, \Lambda_P\}, \\ & 1 \le \Lambda_1 < \ldots < \Lambda_P \le N. \end{aligned} \tag{12}$$

where Λ_{opt} is the set of optimal pilot allocation.

C. DISCUSSION

Unfortunately, the problem in (12) is hard to solve, since we need to exhaust as many as $C(N, P)$ different combinations to search for the global optimum solution. For example, assume $P = 24$ identical pilot symbols are randomly located in a UWA-OFDM system with $N = 512$ subcarriers, the number of exhaustive search is a combination value $C(512, 24) \approx 9.81737 \times 10^{40}$. Even when $P = 16, N = 128$, the result will up to $C(128, 16) \approx 9.33430 \times 10^{19}$, which is also unacceptable for practical calculations due to the high computational complexity and huge time consumption. Therefore, using a method superior to exhaustive search to obtain the optimal pilot allocation quickly is a problem worth investigating.

III. PROPOSED METHODS

The successful application of meta-heuristic optimization algorithms in many fields provides a new approach to solve such optimization problem in (12). In this section, the standard WOA algorithm is modified as a novel variant, namely EWOA. Then, a joint algorithm based on the CS theory and the EWOA algorithm is proposed to optimize pilot allocation for channel estimation in UWA-OFDM systems.

A. PRELIMINARY OF WHALE OPTIMIZATION ALGORITHM (WOA)

In general, the WOA algorithm is composed of three main processes with encircling the prey, bubble attacking of the prey (including shrinking encircling mechanism and spiral updating position), and randomly searching for the prey [21].

In the beginning of WOA, each humpback whale in initial population is set as a search agent, and the target prey is assumed as the current best candidate solution. Once the best search agent is established, the other search agents will approach toward the best one by updating their positions. Define that $\mathbf{W}$ is the position vector of a whale individual, and $\mathbf{W}^*$ denotes the position vector of the target prey. The mathematical model of WOA can be represented by the following equations:

$$\mathbf{S} = \left|\mathbf{C} \cdot \mathbf{W}^*(t) - \mathbf{W}(t)\right| \tag{13}$$

$$\mathbf{W}(t+1) = \mathbf{W}^*(t) - \mathbf{A} \cdot \mathbf{S} \tag{14}$$

where t denotes the current iteration. $\mathbf{A}$ and $\mathbf{C}$ refer to coefficient vectors defined respectively by:

$$\mathbf{A} = 2 \cdot \mathbf{a_0}(t) \cdot \mathbf{r_1} - \mathbf{a_0}(t) \tag{15}$$

$$\mathbf{C} = 2 \cdot \mathbf{r_2} \tag{16}$$

where $\mathbf{r_1}$ and $\mathbf{r_2}$ are random vectors uniformly distributed in the range of (0,1). $\mathbf{a_0}$ is a controlling coefficient linearly decreased from 2 to 0 with iteration times, i.e.

$$\mathbf{a_0}(t) = 2\left(1 - \frac{t}{t_{max}}\right) \tag{17}$$

where t_{max} denotes the maximum number of iterations. Noting that $\mathbf{W}^*$ will be updated in each iteration if there is a better solution.

To describe the bubble-net behavior of humpback whales mathematically, the WOA algorithm achieves the goal of local optimization by shrinking the encircling mechanism and spiral updating position, whose schematic diagrams are illustrated in Fig. 2 and Fig. 3 respectively. Since humpback whales encompass the prey within a shrinking circle and along a spiral-shaped path simultaneously, suppose that there is the same probability of 0.5 to switch between the shrinking of encircling mechanism and the spiral approach to update the position of whales over the iterations when $|\mathbf{A}| < 1$. This process is formulated as follows:

$$\mathbf{S}^* = \left|\mathbf{W}^*(t) - \mathbf{W}(t)\right| \tag{18}$$

$$\mathbf{W}(t+1) = \begin{cases} \mathbf{W}^*(t) - \mathbf{A} \cdot \mathbf{S}, & \lambda_0 < 0.5 \\ \mathbf{S}^* \cdot e^{bl} \cdot \cos(2\pi l) + \mathbf{W}^*(t), & \lambda_0 \geq 0.5 \end{cases} \tag{19}$$

where $\mathbf{S}^*$ indicates the distance of the current whale to the prey, b is a constant for defining the spiral logarithmic shape, l is a random value in $[-1,1]$, and λ_0 is a random switching probability lies in the range of (0,1).

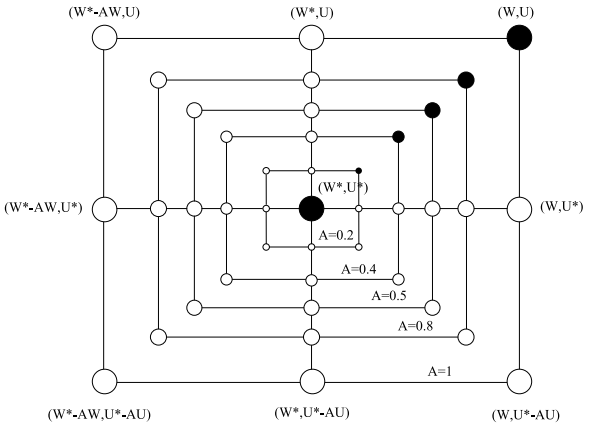

FIGURE 2. Sketch map of shrinking encircling mechanism in WOA. (W^*, U^*) is the position of the current best search agent when $|\mathbf{A}| < 1$. It can be achieved from the search agent (W, U) towards (W^*, U^*) by adjusting the values of A and C [21].

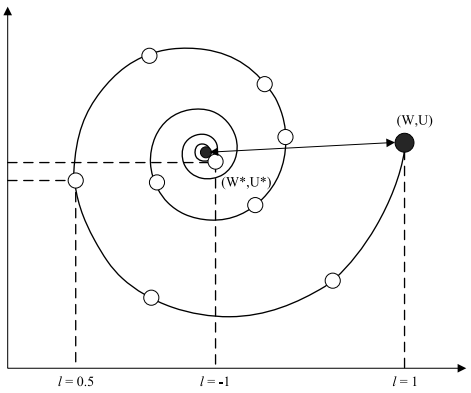

FIGURE 3. Sketch map of spiral updating position in WOA. This approach first calculates the distance between the search agent located at (W, U) and the current best search agent located at (W^*, U^*). A spiral movement is then imitated along a spiral-shaped path between the position of (W, U) and (W^*, U^*) [21].

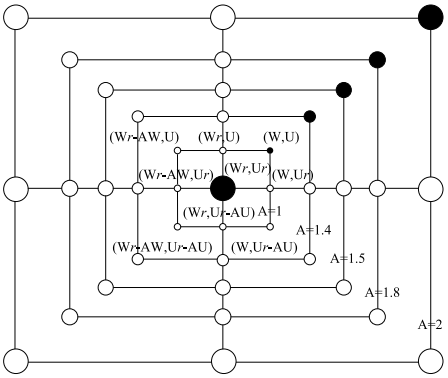

FIGURE 4. Sketch map of randomly search for the prey in WOA. When $|\mathbf{A}| \geq 1$, the position of the search agent $(\boldsymbol{W}, \boldsymbol{U})$ can be replaced by a randomly selected search agent $(\boldsymbol{W_r}, \boldsymbol{U_r})$ from the current population to update the current best search agent [21].

In fact, the whales can also search for the prey randomly according to the position of each other. Therefore, as shown in Fig. 4, when $|\mathbf{A}| \geq 1$, a random search agent is chosen to instead of the best search agent obtained so far to perform a global search, as follows:

$$\mathbf{S}_r = |\mathbf{C} \cdot \mathbf{W}_r(t) - \mathbf{W}(t)| \tag{20}$$

$$\mathbf{W}(t+1) = \mathbf{W}_r(t) - \mathbf{A} \cdot \mathbf{S}_r \tag{21}$$

where $\mathbf{W}_r$ represents a random position vector chosen from the current population.

From the aforementioned description, the WOA algorithm can be considered as a global optimizer, since adaptively tuning of the vectors $\mathbf{A}$ and $\mathbf{C}$ allows WOA to carry out a global search by exploitation ($|\mathbf{A}| < 1$) and exploration ($|\mathbf{A}| \geq 1$). Specifically, only two internal parameters need to be adjusted in the iteration process, which makes WOA a noticeable optimization algorithm.

B. ENHANCED WHALE OPTIMIZATION ALGORITHM (EWOA)

It is similar to many other meta-heuristic algorithms that, WOA may encounter entrapment in local optimum and slow convergence speed when solving practical problems. Therefore, to improve the performance of WOA, a novel algorithm of EWOA is proposed with comprehensive modifications in four perspectives.

1) GOOD POINT SET-BASED INITIALIZATION

Generally speaking, the distribution of the initial population is directly related to the scope of feasible solutions, which will crucially impact on the convergence, search efficiency and stability of WOA. However, the initialization process in WOA is randomly distributed and its coverage space shows great uncertainty. In the case of a limited number of individuals, it may not be able to represent the characteristics of solution space scientifically and adequately, resulting the iterations are easily fell into prematurity.

Good point set (GPS) [58], as a concept of number theory, has been applied in some meta-heuristic algorithms, such as mending the crossover operator in GA algorithm [59], updating the velocity formula for PSO algorithm [60], etc. However, in this work, the method of GPS is adopted to initialize the population and strengthen the ability of individuals for representing the information of solution space. For a R-sized and m-dimensional population, the whale individual $\mathbf{W}_i = \left\{w_i^1, w_i^2, \ldots, w_i^m\right\} (1 \leq i \leq R)$ is initialized by:

$$\begin{cases} \rho \geq 2m+3 & (22) \\ r(j) = 2\cos\left(\dfrac{2\pi j}{\rho}\right), \quad 1 \leq j \leq m & (23) \\ w_i^j = lb_i^j + \mathrm{mod}\left\{r(j)i\right\}(ub_i^j - lb_i^j), \quad 1 \leq i \leq R & (24) \end{cases}$$

where ρ is the minimum prime number subject to (23), mod $\{\cdot\}$ denotes the function of modulo 1, lb and ub are the lower and upper bounds of search space. As a result, $\mathbf{W}_i$ can be regarded as a GPS.

Fig. 5 depicts a two-dimensional example of initialization population by the random and GPS-based methods respectively. Evidently, the population distribution generated by the random method is disorderly and some points overlap markedly. However, the initial population produced by the GPS-based method distributes evenly in the overall solution space without overlapping points and fully characterizes individual diversity to approximate the optimal solution. Furthermore, the construction of GPS is independent with the dimension of solution space, so that it can be well adapted to high-dimensional optimization problems.

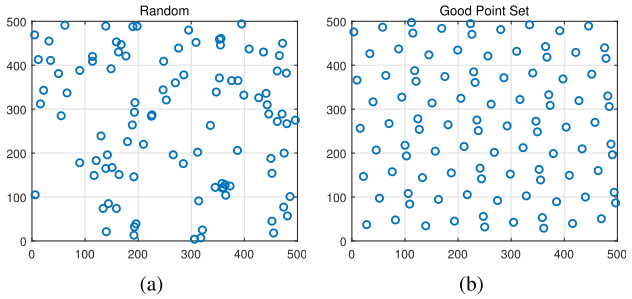

FIGURE 5. Population initialization for a two-dimensional example. (a) Random method. (b) GPS-based method.

2) CHAOTIC SWITCHING PROBABILITY

According to (19), a search agent updates its position with the switching probability λ_0 by choosing between the shrinking encircling method and the spiral model for each iteration in basic WOA algorithm. However, the randomization of λ_0 is usually achieved by using uniform or Gaussian distribution, which may not ensure the each value in the interval of (0,1), especially the boundary values.

Different from WOA, in this paper, an ameliorative switching probability λ is generated by chaotic maps [40], [61], [62] for the randomness, unique ergodicity and non-repetition properties to prevent the search process

from falling into a local minimum. Particularly, the Fuch function, one of chaotic maps, is introduced to implement the switching probability as:

$$\lambda_{t+1} = \cos\left(\frac{1}{\lambda_t^2}\right) \tag{25}$$

where $\lambda_t \in (0, 1)$. The reason for choosing the Fuch function is that, it has stronger chaotic characteristics and more balanced ergodicity than other chaotic functions, e.g., Logistic, Tent, and Chebyshev functions. Since the intervals of chaotic functions and optimization problems are often inconsistent, it is necessary to apply functional transformations and inverse transformations to realize the traversal search of chaotic variables and the calculation of the objective solution values. However, these is no need of functional transformations and inverse transformations for Fuch, which is advantageous to improve the search efficiency in search space. Furthermore, the Fuch function is sensitive to the initial value so that its output will be completely different even given a small change in the initialization. This feature facilitates the Fuch function to avoid trapping into local optimum if the initial setting is improper. Thus, replacing the random distribution of switching probability with the Fuch function helps the EWOA algorithm explore the search space more effectively and globally.

3) NONLINEAR CONTROL PARAMETER

In standard WOA algorithm, the ability to coordinate the exploration and exploitation is of great significance for achieving good searching performance. As mentioned in (19) and (21), the search vector $|\mathbf{A}| \geq 1$ is concentrated on exploring the search space (exploration) and $|\mathbf{A}| < 1$ is dedicated to attacking forward the prey (exploitation). According to (15), the value of $\mathbf{A}$ is determined by the variation of control parameter $\mathbf{a_0}$. Therefore, it can be derived that the balance ability between exploration and exploitation depends on the value of $\mathbf{a_0}$ in fact, which is decreased linearly from 2 to 0 for WOA over the course of iterations.

However, the linear variation cannot appropriately reflect the complicated search process of the WOA algorithm, which may result in low convergence accuracy or prematurity easily. Many studies have indicated that in the early stage of the algorithm, a rapidly changing value of $\mathbf{a_0}$ is beneficial to global search, whereas a slowly changing value is more conducive to local search in the latter stage. For optimizing the control parameter, a number of strategies have been proposed based on the cosine function [63], [64], and chaotic maps [62], etc. Different from these studies, a nonlinear control parameter motivated by the activation function of tanh in neural network [65], [66] is adopted to update the decay during iterations, as given:

$$\mathbf{a}(t) = 2\left[1 - \tanh\left(\frac{3t}{t_{max}}\right)\right] \tag{26}$$

where t and t_{max} denote the current and maximum number of iterations respectively. In this time, the control parameter varies with a nonlinear way from 2 to 0 for balancing the searching ability more effectively in the iteration process.

4) OPPOSITION-BASED LEARNING STRATEGY

As an optimization strategy, opposition-based learning (OBL) [67] has been proved promising to increase the quality of initial population and enhance the performance for meta-heuristic algorithms. The main idea of OBL mechanism is to examine the current solution and its opposite simultaneously for increasing the probability to approach the global best solution [68]. For this work, the OBL strategy is utilized over the iterative process, rather than in the initialization process.

Assume the opposite of the current solution $\mathbf{W}_i$ is defined as $\widetilde{\mathbf{W}}_i = \left\{\widetilde{w}_i^1, \widetilde{w}_i^2, \ldots, \widetilde{w}_i^m\right\}$ $(1 \leq i \leq R)$. Thus, each element in $\widetilde{W}_i$ will be determined according to the OBL strategy:

$$\widetilde{w}_i^j = ub_i^j + lb_i^j - w_i^j, \quad 1 \leq i \leq R, 1 \leq j \leq m \tag{27}$$

where $w_i^j \in [lb_i^j, ub_i^j]$. In each iteration, the current best solution can be attained after all the search agents update their positions. Then, OBL is employed to generate the opposite of this current best solution in this work. To select the global best solution, the fitness value of the current best solution and its opposite in the search space will be calculated by:

$$\mathbf{W}^* = \begin{cases} \mathbf{W}_i, & if\ F(\mathbf{W}_i) \leq F(\widetilde{\mathbf{W}}_i) \\ \widetilde{\mathbf{W}}_i, & if\ F(\mathbf{W}_i) > F(\widetilde{\mathbf{W}}_i) \end{cases} \tag{28}$$

where $F(\cdot)$ is the fitness function. Therefore, introducing OBL strategy is advantageous to expand the diversity of the search population and optimize the search process, so that the evolutionary search agent can converge to the global optimal solution more quickly.

Comprehensively, the proposed EWOA benefits from the GPS-based initialization, chaotic switching probability, nonlinear control parameter, and OBL strategy for achieving better performance on solution accuracy, searching reliability, and convergence speed. Moreover, it is worth noting that EWOA retains the framework of the standard WOA algorithm and it does not introduce additional parameters that need to be adjusted in the iteration process. The flowchart of the proposed EWOA algorithm is presented in Fig. 6.

C. JOINT CS-EWOA METHOD

In traditional optimization methods, random search is routinely used to seek the optimal pilot allocation based on the CS theory for channel estimation in UWA-OFDM systems. This study replaces the random search method with the proposed EWOA algorithm to address the pilot allocation problem more efficiently.

To adapt to the optimization problem of pilot allocation, it is necessary to specifically redefine the relevant parameters in EWOA. Each whale individual (search agent) in R-sized initial population is denoted by m-dimensional position vector as $\mathbf{W}_i = \left\{w_i^1, w_i^2, \ldots, w_i^m\right\}$ $(1 \leq i \leq R)$. The vector dimensions from 1 to m correspond to the positions of pilot symbols, where the value of m equals the number

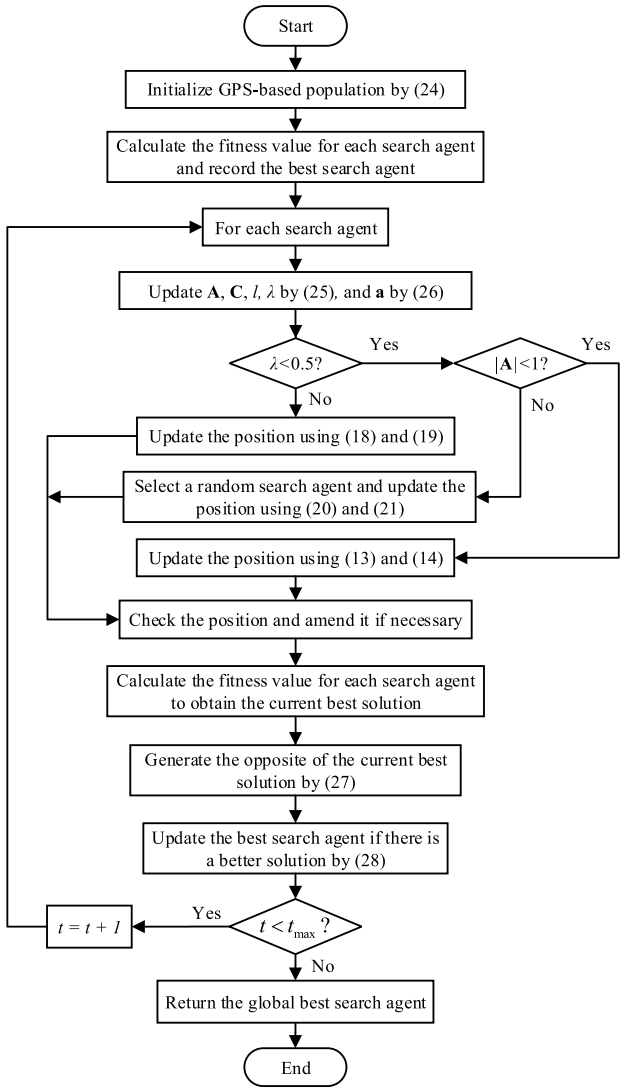

FIGURE 6. The flowchart of the proposed EWOA algorithm.

of pilot symbols P numerically. Consequently, optimizing pilot allocation is essentially to optimize the dimensions of position vectors. In this paper, the values of each position vector are restricted with non-repetitive positive integers in the range of $[1, N]$, where N is the number of total subcarriers in UWA-OFDM systems. Position values of each search agent will be rounded to the nearest integers if necessary. After each update, if a search agent goes beyond the boundaries of the search space or contains duplicate integers in its position vector, the CS-EWOA algorithm will replace this illegal search agent with a new random one. On the one hand, randomly selecting a new search agent equals to performing a random search for the prey as shown in Fig. 4, which conforms to the search mechanism of EWOA algorithm; on the other hand, this operation increases the diversity of individuals in a manner, which is conducive to global search for the best solution. Moreover, it introduces almost no additional time and resource consumption. The fitness function of this optimization problem is defined to calculate the mutual coherence in (11):

$$F_{fitness} = \mu(\mathbf{D}) \tag{29}$$

In this paper, a joint algorithm termed CS-EWOA is proposed for pilot allocation optimization, combining the CS theory with the EWOA algorithm. The pseudo code of CS-EWOA is described in Algorithm 1. As shown, it is comprised of three phases, successively as initialization (Phase-I), pilot allocation optimization (Phase-II), and performance evaluation (Phase-III). First of all, the simulation parameters, such as the numbers of subcarriers N and pilot symbols P for UWA-OFDM systems, the population size R, vector dimension m and the maximum iteration number t_{max} for the EWOA algorithm, are initialized in Phase-I as well as the generation of whales population. Later on, the optimization problem of pilot allocation as indicated in (12) is handled by the iterations of whale population. During the main loop, it starts with evaluating the fitness function in (29) and terminates by t_{max} to select the global best solution $\mathbf{W}^*$ as the optimal pilot allocation for UWA-OFDM systems. In the last phase, after generating the measurement matrix with the aid of $\mathbf{W}^*$, the performance of this joint algorithm will be measured based on the CS framework in view of BER and MSE versus signal to noise ratio (SNR) quantitatively.

IV. SIMULATION RESULTS AND ANALYSIS

In this section, extensive simulations are performed to validate the proposed EWOA algorithm as well as evaluate the performance of the joint CS-EWOA pilot allocation algorithm for channel estimation in UWA-OFDM systems. All simulations are implemented in MATLAB R2018a and run on Windows 7 operative system with 64-bit support using an Intel Core i7 CPU at 3.60 GHz and 8 GB of RAM.

A. BENCHMARK TESTING FOR EWOA

To verify the improvement of the proposed EWOA algorithm on optimization capability over the standard WOA algorithm, twelve classical benchmark functions in [20] are selected at first to examine the performance mathematically. In general, these benchmark functions are designed to test meta-heuristic methods from various perspectives. As shown in Table 1, functions F1 to F6 are high-dimension unimodal used to test the ability of exploitation and convergence, whereas F7 to F12 are high-dimension multimodal used to test the ability of exploration and evading local optimum. Here, *Dim*, *Range*, and F_{min} refer to the dimension, boundary of search space, and theoretical minimum for each benchmark function respectively.

Meanwhile, six representative meta-heuristic algorithms are also compared with WOA and EWOA algorithms, which are GA [26], PSO [32], moth-flame optimization algorithm (MFO) [69], hybrid PSO and gravitational search algorithm (PSOGSA) [70], BA [19], and ABC [18]. The parameters of these considered meta-heuristic algorithms are given

Algorithm 1 Proposed CS-EWOA Pilot Allocation Algorithm

% Phase-I: initialization
Define the simulation parameters for the UWA-OFDM system with N, P, and also for the WOA algorithm with R, m, t_{max}, where $m = P$.
Initialize the whales population by GPS-based method in (24), and the elements of each whale $\mathbf{W}_i$ are non-repetitive positive integers belonging to the lower and upper bounds of $[1, N]$.
% Phase-II: pilot allocation optimization
Calculate the fitness value defined in (29) for each search agent.
Record the optimal fitness value and the corresponding search agent $\mathbf{W}^*$ as the best search agent.
$t = 0$.
while ($t < t_{max}$)
  for $i = 1$ **to** R **do**
    Update the parameters $\mathbf{A}$, $\mathbf{C}$, l, λ by (25) and $\mathbf{a}$ by (26).
    if ($\lambda < 0.5$)
      if ($|\mathbf{A}| < 1$)
        Update the position of the current search agent by (13) and (14).
      else if ($|\mathbf{A}| \geq 1$)
        Select a random search agent $\mathbf{W}_r$.
        Update the position of the current search agent by (20) and (21).
      end if
    else if ($\lambda \geq 0.5$)
      Update the position of the current search agent by (18) and (19).
    end if
  end for
  Check the position of each search agent in current population.
  if (the search agent goes beyond the boundaries of the search space **or** exists duplicate positive integers)
    Replace it with a new random search agent.
  else
    Retain the original search agent.
  end if
  Calculate the fitness value for each updated search agent to obtain the current best solution.
  Generate the opposite $\widetilde{\mathbf{W}}_i$ of the current best solution by the OBL strategy in (27).
  Update the $\mathbf{W}^*$ if there is a better solution by (28).
  $t = t + 1$.
end while
Return the global optimal value of fitness function and the corresponding search agent $\mathbf{W}^*$ that is also the optimal solution to the optimization problem in (12).
% Phase-III: performance measurement
Generate the measurement matrix $\mathbf{D}$ in (7) based on $\mathbf{W}^*$.
Recover the sparse CIR vector $\mathbf{h}$ in (8) with greedy reconstruction algorithms by the CS theory.
Evaluate the channel estimation performance for UWA-OFDM systems on BER and MSE versus SNR criteria.

in Table 2, wherein part of them are derived from the literature [41]. For the sake of fairness, all algorithms are set with the same population size of 20 and maximum iteration number of 1000. A number of 30 repetitive runs are conducted independently to eliminate the impact of contingency.

As reported in Table 3 and Table 4, the statistical results are obtained in terms of *Best*, *Worst*, *Mean*, and *Std* for 12 benchmark functions, denoting the best value, the worst value, the average value and the standard deviation of overall results in 30 runs, respectively. For each benchmark function, the optimal values of *Mean* attained by different algorithms are highlighted in bold. It can be observed from Table 3 and Table 4 that the EWOA algorithm can provide quite competitive performance on these 12 benchmark functions. On the one hand, for the unimodal functions from F1 to F6, it outperforms all other seven algorithms with far less values of *Mean*. On the other hand, EWOA shows better optimization results than the others for the multimodal functions from F7 to F11, except for F12 in which the BA algorithm gets the best solution. Especially, the proposed EWOA algorithm achieves the theoretical optimal value of zero for F8 and F10 functions.

In addition, T-test is established to measure the significance different between the proposed EWOA and the

TABLE 1. Details of classical benchmark functions.

No.	Name	Test function	Dim	Range	F_{min}
F1	Sphere	$f(x)=\sum_{i=1}^{n} x_i^2$	50	[-100,100]	0
F2	Schwefel 2.22	$f(x)=\sum_{i=1}^{n} \lvert x_i\rvert + \prod_{i=1}^{n} \lvert x_i\rvert$	50	[-10,10]	0
F3	Schwefel 1.2	$f(x)=\sum_{i=1}^{n} \left(\sum_{j=1}^{i} x_j\right)^2$	50	[-100,100]	0
F4	Schwefel 2.21	$f(x)=\max_i \{\lvert x_i\rvert, 1\le i\le n\}$	50	[-100,100]	0
F5	Resonbrock	$f(x)=\sum_{i=1}^{n-1} \left[100\left(x_{i+1}-x_i^2\right)^2+(x_i-1)^2\right]$	50	[-30,30]	0
F6	Step	$f(x)=\sum_{i=1}^{n} (\lvert x_i+0.5\rvert)^2$	50	[-100,100]	0
F7	Alpine	$f(x)=\sum_{i=1}^{n} \lvert x_i \sin(x_i)+0.1x_i\rvert$	50	[-10,10]	0
F8	Rastrigin	$f(x)=\sum_{i=1}^{n} \left[x_i^2-10\cos(2\pi x_i)+10\right]$	50	[-5.12,5.12]	0
F9	Ackley	$f(x)=-20\exp\left[-0.2\sqrt{\frac{1}{n}\sum_{i=1}^{n} x_i^2}-\exp\left(\frac{1}{n}\sum_{i=1}^{n}\cos 2\pi x_i\right)\right]+20+e$	50	[-32,32]	0
F10	Griewank	$f(x)=\frac{1}{4000}\sum_{i=1}^{n}\left(x_i^2\right)-\prod_{i=1}^{n}\cos\left(\frac{x_i}{\sqrt{i}}\right)+1$	50	[-600,600]	0
F11	Penalized 1	$f(x)=\frac{\pi}{n}\left\{10\sin(\pi y_1)+\sum_{i=1}^{n-1}(y_i-1)^2\left[1+10\sin^2(\pi y_{i+1})\right]+(y_n-1)^2\right\}$ $+\sum_{i=1}^{n}\mu(x_i,10,100,4)$ $y_i=1+\frac{x_i+1}{4}$ $\mu(x_i,a,k,m)=\begin{cases} k(x_i-a)^m, x_i>a \\ 0, -a<x_i<a \\ k(-x_i-a)^m, x_i<-a \end{cases}$	50	[-50,50]	0
F12	Zakharov	$f(x)=\sum_{i=1}^{n} x_i^2+\left(\sum_{i=1}^{n} 0.5ix_i\right)^2+\left(\sum_{i=1}^{n} 0.5ix_i\right)^4$	50	[-5,10]	0

others algorithms. The marks of plus (+), minus (−) and equal sign (=) indicate that the result obtained by EWOA algorithm is better than, worse than, or equivalent to that obtained by the corresponding algorithm in the double-tailed T-test with significance level of 5% respectively. Then, *Score* represents the number of benchmark functions in which EWOA is significantly superior to the corresponding algorithm. It is, namely, the subtraction of the plus and minus signs. This statistical test is critical to prove that the proposed EWOA algorithm achieves a significant improvement compared to other meta-heuristic algorithms. According to the *Score* of T-test from Table 4, EWOA offers the best global solutions on 10 out of 12 functions for GA, PSO, BA algorithms, 11 out of 12 functions for WOA algorithm, and 12 out of 12 functions for MFO, PSOGSA, ABC algorithms. It obviously illustrates that the proposed EWOA algorithm performs better than the others regarding convergence accuracy and local optimum avoidance on the majority of the benchmark functions. Specifically, EWOA shows similar performance for F9 and superior performance for all the remaining benchmark functions in comparison with the standard WOA algorithm. From these analysis results, it can be confirmed that the EWOA algorithm is effectively improved by our optimization strategies on the ability of exploration and exploitation.

B. PERFORMANCE FOR CHANNEL ESTIMATION

In this subsection, our proposed joint CS-EWOA pilot allocation algorithm is applied to UWA-OFDM systems and compared with the equispaced, random, GA, PSO and WOA based methods for channel estimation performance on BER and MSE versus SNR criteria.

To imitate the underwater communication environment more realistically, the BELLHOP ray model [71]–[73] is employed to establish the UWA multipath channel with actual ocean data. The considered underwater region is in the South China Sea, located at a latitude and longitude of 24.2874 and 119.3469 degree, respectively. BELLHOP takes account of the sound speed profile (SSP), boundaries of sea surface and bottom, interface reflecting and scattering, and geometry of the transmitter and receiver. As shown in Fig. 7(a), the water depth is approximately 100 meters, and the transmitter and receiver are placed 1000 meters apart at the same depth of 30 meters. In our simulations, the sea surface and bottom are modeled with the real data obtained from AVISO$^+$ [74] and Google Map API [75], respectively. As a function of water temperature, salinity and depth, the actual SSP data in Fig. 7(b) are measured on June 21, 2013 from the database of World Ocean Atlas 2013 (WOA13) [76], decreasing from 1540 m/s at the water surface to 1512 m/s at the bottom. Moreover, the attenuation coefficient and

TABLE 2. Parameterization for the considered meta-heuristic algorithms.

Algorithm	Parameter	Value
GA [26]	Population size	20
	Number of iteration	1000
	Crossover rate	0.7
	Mutation rate	0.006
	Generation gap	0.9
PSO [32]	Population size	20
	Number of iteration	1000
	Cognitive factor	1.5
	Social factor	2.0
	Maximum velocity	10
	Inertia Weight	1
	Damping Ratio	0.99
MFO [69]	Population size	20
	Number of iteration	1000
	Convergence constant	linearly decreased from -1 to -2
PSOGSA [70]	Population size	20
	Number of iteration	1000
	Weighting factor c_1	0.5
	Weighting factor c_2	1.5
	Initial value G_0	1
	Random number ω	[0,1]
BA [19]	Population size	20
	Number of iteration	1000
	Loudness A	0.9
	Pulse emission rate r	0.5
	Fixed frequency f	[-1,1]
ABC [18]	Population size	20
	Number of iteration	1000
	Limit percentage	50%
WOA [21]	Population size	20
	Number of iteration	1000
	Control coefficient $\mathbf{a_0}$	linearly decreased from 2 to 0
EWOA [ours]	Population size	20
	Number of iteration	1000
	Optimization strategies	according to (24) - (27)

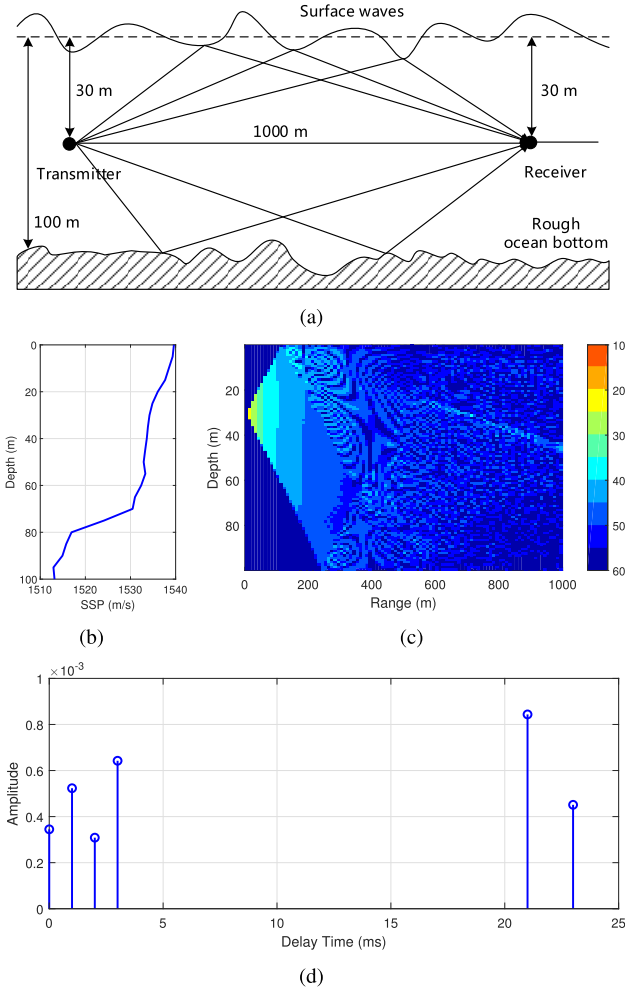

FIGURE 7. BELLHOP ray model of a shallow UWA multipath channel in South China Sea. (a) Schematic diagram of eigenray propagation. (b) Measured SSP values versus depths. (c) Predicted transmission loss versus depths and ranges with a source at 30 m depth. (d) Deterministic CIR for a multipath sparse channel.

density of the sediment layer are 0.8 dB/λ and 1.9 g/cm^3, respectively. After all these environmental profiles are input to BELLHOP model, it produces a variety of useful outputs such as eigenrays, transmission loss, arrival time-series and amplitudes, etc. Fig. 7(c) predicts the transmission loss with respect to different depths and ranges. In particular, the CIR, showing in Fig. 7(d), is clustered by six taps with dominated powers at the receiver. The multipath delays and gains are [0, 1, 2, 3, 21, 23] ms and [-34.6, −32.8, −35.1, −31.9, −30.7, −33.5] dB for each tap respectively. Taking the obtained CIR vector as an initial value, a time-varying fading channel is modeled as obeying the statistical characteristics of Rayleigh distribution [77]. Meanwhile, in this so-called specific channel model, the Doppler scaling factors associated with different paths are chosen randomly from a zero mean uniform distribution within [−0.003, 0.003] according to [78]. As stated above, the UWA channel is accomplished by combining BELLHOP with statistical characteristics of the measured channels. Similar channel models have been widely researched and applied in many literatures [7], [46]–[50], [79]. Consequently, the simulated UWA channel is able to support the reliability and stability of our proposed algorithm with different conditions in underwater communication environments.

For the following emulations, a UWA-OFDM system with $N = 256$ subcarriers is simulated to estimate the performance of various pilot allocation methods. The system parameters are appointed in Table 5. Note that, the number of pilot subcarriers in UWA-OFDM system is set to $P = 24$, which is four times the channel sparsity of $K = 6$ according to the measurement requirements of CS theory [80]. Here, quadrature phase shift keying (QPSK) constellation modulates the transmission signal and the widespread OMP algorithm [51] is applied to reconstruct the sparse CIR vector for these pilot

TABLE 3. Performance comparisons of optimization algorithms on benchmark functions (F1 to F10).

Function	Results	Optimization algorithm							
		GA [26]	**PSO** [32]	**MFO** [69]	**PSOGSA** [70]	**BA** [19]	**ABC** [18]	**WOA** [21]	**EWOA** [ours]
F1	Best	116.8437389	0.58243993	6.1500000	1.8000000	58700.00	0.0066133	2.2864E-152	4.8049E-301
	Worst	572.4468734	198.674038	20000.000	40000.000	93300.00	0.8727587	8.3934E-128	4.9904E-263
	Mean	381.3589181	16.6944096	6656.1400	7680.0000	76649.85	0.1613981	3.2703E-129	**1.6635E-264**
	Std	114.3406925	36.6897375	7500.0000	10100.000	8760.000	0.2239980	1.5420E-128	0
	T-test	+	+	+	+	+	+	+	
F2	Best	4.852204706	0.868909712	0.7180000	0.0799229	2.32E+11	0.0404188	1.0120E-108	2.8383E-231
	Worst	11.15352293	7.375803792	120.03400	218.73276	4.75E+21	0.1881228	1.2831E-93	4.4653E-205
	Mean	7.721199799	3.241994553	63.600000	109.00000	1.70E+20	0.0905261	5.9643E-95	**1.4884E-206**
	Std	1.685157964	1.451478860	32.600000	74.420650	8.66E+20	0.0380328	2.4797E-94	0
	T-test	+	+	+	+	+	+	+	
F3	Best	17513.50854	1178.970240	25488.4152	17205.387	48187.3460	39802.975	113426.7294	3.6584E-02
	Worst	34047.72031	6410.659931	119231.193	65464.000	2719113.27	71824.640	252770.1226	2.7603E-01
	Mean	25452.36192	3018.095674	52969.0978	37602.818	129706.970	54842.006	172240.8117	**1.4292E-01**
	Std	4506.036946	1442.639746	23032.2545	14127.625	49529.6800	8250.2000	35258.04188	6.7284E-02
	T-test	+	+	+	+	+	+	+	
F4	Best	13.66077457	5.965451115	77.5100663	43.845901	69.714887	72.037700	0.014750763	1.6105E-37
	Worst	22.20820023	14.21977989	92.3926922	96.120853	83.529828	86.990567	94.26879073	64.342000
	Mean	18.12956455	9.508099589	87.4935800	76.242645	77.279800	81.701450	65.93399891	**2.7645000**
	Std	2.172751320	2.116438479	4.09000000	15.956892	3.4000000	3.3201720	27.81716205	12.016000
	T-test	+	+	+	+	+	+	+	
F5	Best	6193.579465	144.7309563	5270.00000	113.52291	262000.00	171.41463	47.08115317	0.45311860
	Worst	33201.10122	6881.983903	241459526	15988931	5384803.4	2579.3251	48.65486794	46.3797272
	Mean	20066.49581	1264.721107	27016318.9	21186373	2538617.0	738.48054	47.97827057	**41.2074420**
	Std	7507.439993	1647.816234	64227209.8	46205843	1240403.9	523.85824	0.537449500	13.7332721
	T-test	+	+	+	+	+	+	+	
F6	Best	242.2403707	0.445958757	2.47997406	0.2597229	633858.78	0.0105582	0.377773869	2.1206E-03
	Worst	545.6944292	273.0729831	31900.0000	29700.000	98100.000	1.2641610	2.602022344	7.1839E-03
	Mean	381.1813594	25.97757696	8330.00000	6330.9504	78500.000	0.1287937	1.408544176	**4.4706E-03**
	Std	81.37228885	58.59860246	8168.76401	7630.1711	8131.8392	0.2384516	0.651896864	1.4383E-03
	T-test	+	+	+	+	+	+	+	
F7	Best	2.819770272	0.191369758	0.49575720	3.4273133	9.0027522	0.0715158	1.0470E-107	8.3980E-264
	Worst	11.46117480	2.218377216	32.0813744	22.389674	44.380242	0.6720755	2.1045E-88	8.8566E-243
	Mean	6.348339803	0.987402120	12.3003329	11.239291	20.171644	0.3005940	7.0149E-90	**5.1644E-244**
	Std	2.171454264	0.551644006	8.67722171	5.5162568	8.0592873	0.1476362	3.8422E-89	0
	T-test	+	+	+	+	+	+	+	
F8	Best	110.2502617	50.86871663	268.831115	175.11227	288.38874	11.126150	0	0
	Worst	246.0060332	145.0485000	450.000000	381.06687	466.00000	24.279880	5.68434E-14	0
	Mean	154.0825550	100.8730755	334.000000	279.11064	371.00000	17.000000	1.89478E-15	**0**
	Std	29.94267253	21.97486661	52.5572791	54.156122	41.240335	2.8910441	1.03781E-14	0
	T-test	+	+	+	+	+	+	+	
F9	Best	3.652379746	2.461948322	18.4375531	16.061921	18.860989	0.1793727	8.8818E-16	8.8818E-16
	Worst	5.734156460	5.218268815	20.0000000	20.000000	19.900000	1.3257102	7.9936E-15	7.9936E-15
	Mean	4.657614856	3.542686000	19.5586102	18.510762	19.391349	0.8037350	**4.7962E-15**	**4.4409E-15**
	Std	0.461062808	0.705810282	0.46043749	0.8579219	0.3195088	0.3440640	2.6960E-15	2.7990E-15
	T-test	+	+	+	+	+	+	=	
F10	Best	2.457532664	0.232669456	1.08783843	1.2700000	817.00000	0.0101887	0	0
	Worst	7.520921324	3.126774671	271.309496	183.75765	1202.7643	0.5818773	0.201708839	0
	Mean	4.682245125	1.026349406	44.0597501	80.711588	1061.1506	0.1491764	0.006723628	**0**
	Std	1.033084119	0.572724218	65.6000000	72.756241	87.370446	0.1182633	0.036826827	0
	T-test	+	+	+	+	+	+	+	

TABLE 4. Performance comparisons of optimization algorithms on benchmark functions (F11 to F12).

Function	Results	Optimization algorithm							
		GA [26]	**PSO** [32]	**MFO** [69]	**PSOGSA** [70]	**BA** [19]	**ABC** [18]	**WOA** [21]	**EWOA** [ours]
F11	Best	0.795415329	0.577878238	7.72233888	13.774878	8861228	0.0003427	0.006750429	3.3298E-04
	Worst	3.403151663	14.65139536	512025046	51200006	48304869	0.0497181	0.092192110	1.1594E-03
	Mean	2.154487482	3.858896810	172000000	59700000	25300000	0.0099176	0.031731519	**7.5559E-04**
	Std	0.691254562	2.944963162	93455862.3	12902576	11358203	0.0133278	0.021677958	2.1158E-04
	T-test	+	+	+	+	+	+	+	
F12	Best	200.8072570	244.6182900	428.529327	249.31637	32.194495	918.48678	661.2046420	185.710461
	Worst	517.7033287	672.7066200	2107.76072	988.12786	442.13725	1312.8759	1010.991031	882.170805
	Mean	315.2169252	429.8948700	1258.84177	522.62671	**78.612517**	1166.1103	854.7215461	494.358997
	Std	73.75424894	99.96015400	465.875760	210.10237	80.290840	93.132404	86.52437432	169.644390
	T-test	-	-	+	+	-	+	+	
Better (+)		11	11	12	12	11	12	11	
Same (=)		0	0	0	0	0	0	1	
Worse (-)		1	1	0	0	1	0	0	
Score		10	10	12	12	10	12	11	

TABLE 5. Simulation parameters of the UWA-OFDM system.

Parameter	Value
Carrier frequency (f_c)	10 kHz
Channel bandwidth (B)	2 kHz
Number of subcarriers (N)	256
Size of FFT/IFFT	256
Subcarriers spacing (Δf)	7.81 Hz
OFDM symbol duration (T)	160 ms
Cyclic prefix duration (T_{cp})	32 ms
Sparsity of channel model (K)	6
Number of pilot symbols (P)	24
Length of channel model (L)	50
Noise model	Additive White Gaussian Noise

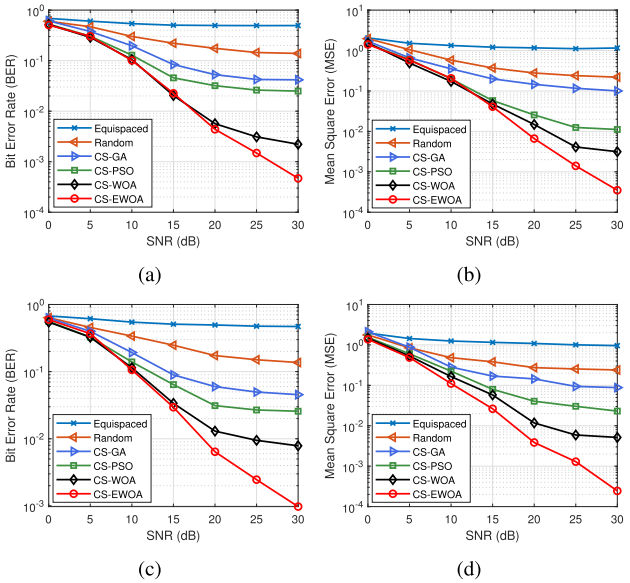

FIGURE 8. Performance comparisons on BER and MSE versus SNR for various pilot allocation methods over the specific channel model. (a) BER for $N = 256$. (b) MSE for $N = 256$. (c) BER for $N = 512$. (d) MSE for $N = 512$.

allocation methods. It is assumed that the Doppler spreads for each path are perfectly evaluated and compensated at the receiver. Furthermore, parameterizations of the selected CS-GA, CS-PSO, CS-WOA, and the proposed CS-EWOA optimizers are the same as defined in Table 2, except for the numbers of population size and iteration time. In this case, these two parameters are set to $R = 100$ and $t_{max} = 200$ respectively. Working with the same conditions aims to counteract the unnecessary effects caused by different parameter values in performance comparisons.

Through 1500 Monte Carlo trials, BER and MSE of different pilot allocation methods over the specific channel model for 256 subcarriers are presented in Fig. 8(a) and 8(b), respectively. It can be seen that our proposed CS-EWOA algorithm outperforms the other considered pilot allocation methods by achieving both the best BER and MSE performance. Contrarily, the equispaced method shows the worst performance, in which its BER and MSE curves hardly decrease with the increase of SNR. Since pilot allocations directly determine the composition of the measurement matrix, equispaced pilots produce a measurement matrix with a large value of mutual coherence, resulting to a poor sensing property by the strongly correlated matrix entries. Unfortunately, this measurement matrix cannot fit well with the RIP condition, which seriously degrades the estimation accuracy of the reconstruction algorithm [8], [12], [78]. In the CS-EWOA algorithm, however, the measurement matrix is generated with a very small mutual coherence through evolutionary iterations. As a result, it makes the CS-EWOA algorithm obtain much better channel estimation performance. Therefore, the equispaced pilot allocation is no longer applicable to the CS-based channel estimation

whereas it is actually optimal in traditional estimation methods, such as LS, MMSE. For the random method, the BER and MSE performance are slightly better than the equispaced one. Three meta-heuristic based optimization algorithms, CS-GA, CS-PSO, and CS-WOA, are superior to the equispaced and random ones, but still inferior to the proposed CS-EWOA algorithm. Although the performance advantage of CS-EWOA algorithm over other methods is not particularly prominent at lower SNR values between 0 dB and 10 dB, it becomes more and more apparent as the SNR increases from 15 dB to 30 dB. For instance, in Fig. 8(a), at the SNR value of 30 dB, BERs of the equispaced, random, CS-GA, CS-PSO, CS-WOA, and CS-EWOA methods are 4.9×10^{-1}, 1.4×10^{-1}, 4.2×10^{-2}, 2.5×10^{-2}, 2.2×10^{-3}, and 5.0×10^{-4}, respectively. In Fig. 8(b), we can observe that the trend of MSE performance is consistent with that of BER for each considered method. As shown, the performance difference of MSE between CS-EWOA with 4.0×10^{-4} and its closest CS-WOA with 3.1×10^{-3} is approximately 10^{-1} at 30 dB SNR.

To investigate the effect of a higher number of subcarriers on system performance, the simulations are also carried out for 512 subcarriers with 24 pilot symbols. Fig. 8(c) and 8(d) depict the performance comparisons among the considered pilot allocation methods in terms of BER and MSE criteria over the specific channel model, respectively. Clearly observing from the figures, the proposed CS-EWOA algorithm maintains the accordant performance of BER and MSE as obtained in Fig. 8(a) and 8(b) for 256 subcarriers. It means even though the number of system subcarriers is escalated from 256 to 512, CS-EWOA does not lose its performance superiority on both BER and MSE.

Furthermore, to validate the robustness of our proposed CS-EWOA algorithm over different UWA channels, we model a series of UWA multipath channels as previously, termed as the dynamic channel model. The sparsity level is fixed to $K = 6$, but the positions of the non-zero taps are random for each channel. it is hypothesized that the arrival time intervals of multipaths distribute exponentially with a mean of 1 ms, and the amplitudes are Rayleigh distributed with the average power, which decays exponentially with the time delay [8], [78]. Similar to the specific channel model, UWA-OFDM systems with 256 and 512 subcarriers are implemented with 1500 Monte Carlo trials respectively in this case. The BER and MSE curves of channel estimation performance for each pilot allocation method are exhibited in Fig. 9. According to the figure, the proposed CS-EWOA algorithm keeps its strong robustness by still presenting the best performance on BER and MSE in comparison with the equispaced, random, CS-GA, CS-PSO, and CS-WOA methods, for both different system subcarriers. The result reveals that the proposed CS-EWOA algorithm is robust against different UWA channel environments.

Comparing to the Fig. 8 and 9, the performance on BER and MSE of six pilot allocation methods are examined in different system subcarriers and types of channel models.

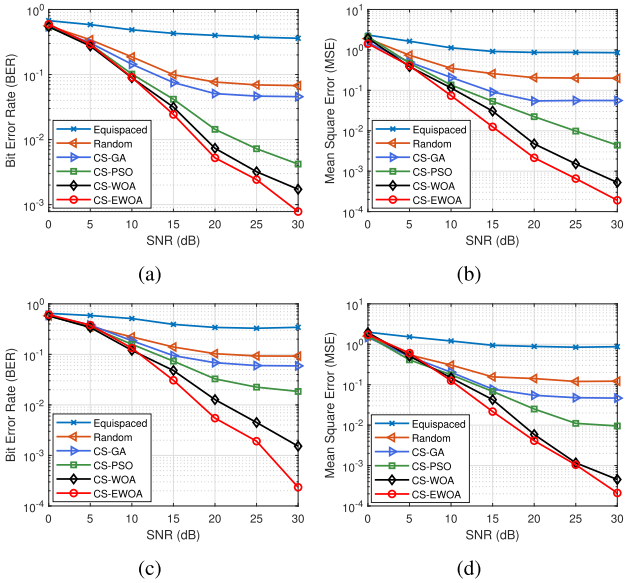

FIGURE 9. Performance comparisons on BER and MSE versus SNR for various pilot allocation methods over the dynamic channel model. (a) BER for $N = 256$. (b) MSE for $N = 256$. (c) BER for $N = 512$. (d) MSE for $N = 512$.

The robusticity and validity of the proposed CS-EWOA algorithm are demonstrated by its consistent and superior performance over other considered methods in each simulation.

C. CONVERGENCE ANALYSIS

The convergence performance of CS-EWOA is compared with three meta-heuristic algorithms of CS-GA, CS-PSO, and CS-WOA. Based on the simulations in the previous subsection, the curves of fitness value for the specific channel model with 256 and 512 subcarriers are illustrated in Fig. 10(a) and 10(b), as well as that for the dynamic channel model with 256 and 512 subcarriers are illustrated in Fig. 10(c) and 10(d), respectively.

With a view to convergence accuracy, as it can be seen from each figure, the iterative convergence of the CS-EWOA algorithm outperforms the CS-GA, CS-PSO, and CS-WOA algorithms with lower fitness value when the maximum iteration is finished. CS-WOA follows the CS-EWOA, and CS-PSO is inferior to CS-WOA but superior to CS-GA. More intuitively, the final fitness values of the considered pilot allocation methods for different simulation scenarios are recorded in Table 6. For instance, if the attention is paid to the dynamic channel model with 512 subcarriers in Table 6, the meta-heuristic based algorithms CS-EWOA, CS-WOA, CS-PSO, and CS-GA achieve better fitness values than the equispaced method with 0.8751 and the random method with 0.6414, whereas such value of CS-EWOA is as low as 0.2141, superior to CS-WOA with 0.2153, CS-PSO with 0.2267 and CS-GA with 0.2770.

For convergence speed, if we observe the convergence curve in Fig. 10 carefully, it can be found that the CS-GA and CS-PSO algorithms perform poorly because they are easy to suffer from premature phenomena, especially in Fig. 10(b).

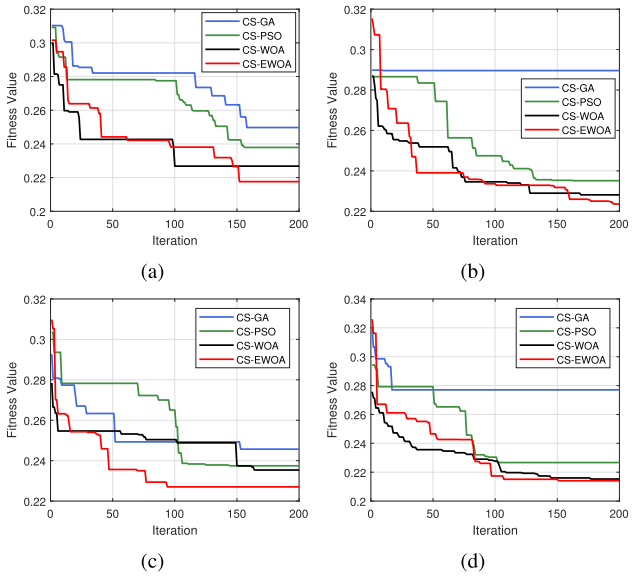

FIGURE 10. Convergence curves of various optimization algorithms in different conditions. (a) The specific channel model with $N = 256$. (b) The specific channel model with $N = 512$. (c) The dynamic channel model with $N = 256$. (d) The dynamic channel model with $N = 512$.

TABLE 6. Final fitness values of various pilot allocation methods.

Algorithm	Specific channel model		Dynamic channel model	
	$N = 256$	$N = 512$	$N = 256$	$N = 512$
Equispaced	0.8751	0.8751	0.8751	0.8751
Random	0.6457	0.6133	0.6128	0.6414
CS-GA	0.2497	0.2896	0.2457	0.2770
CS-PSO	0.2379	0.2351	0.2375	0.2267
CS-WOA	0.2268	0.2281	0.2354	0.2153
CS-EWOA	0.2176	0.2236	0.2270	0.2141

The reason is that, only one formula is generally utilized for CS-GA and CS-PSO to update the positions in each iteration, resulting to reduce the diversity of individuals in the population and increase the occurrence possibility of being trapped locally. However, CS-WOA and CS-EWOA outperform CS-GA and CS-PSO by displaying faster convergence curves, especially at the very beginning of the iteration process. Due to the distinctive position updating mechanism of search agents, it endows the CS-WOA and CS-EWOA algorithms with a better equilibrium ability for local exploitation and global exploration. Meanwhile, the optimization strategies further reinforce the convergence performance for the proposed CS-EWOA algorithm over CS-WOA. As shown, CS-EWOA declines throughout the overall iterations to effectively avoid falling into local optimum and accelerates the convergence process to ensure better global solutions.

D. COMPUTATIONAL COMPLEXITY ANALYSIS

In this part, rough computational complexities of the metaheuristic based algorithms CS-GA, CS-PSO, CS-WOA, and CS-EWOA are investigated to evaluate the system performance. Since all these four algorithms work with the same fitness function of (29) in the framework of CS theory, we only compare the computational complexity of the optimization process for pilot allocation. The analysis is made with the population size R, the dimension m, and the number of iterations t_{max} for convergence.

In CS-WOA algorithm, the computational complexity is mainly reflected in the population initialization and iteration process. First of all, the complexity order of population initialization is $O(R{\cdot}m)$. Then, during the main iteration process, all search agents in population are required to update their current position and compare their current fitness value with the individual best as well as the global best, resulting in a complexity order of $O(R{\cdot}m{\cdot}t_{max})$. According to the derivation rules of complexity, therefore, the computational complexity of CS-WOA algorithm can be recorded as $O(R{\cdot}m{\cdot}t_{max})$. Similarly, the computational complexities of CS-GA and CS-PSO are $O(R{\cdot}g{\cdot}t_{max})$ and $O(R{\cdot}d{\cdot}t_{max})$ respectively, where g and d denote the length of genotypes and the number of additional operations for adjusting the position of particles [25], [28]. As described above, the proposed CS-EWOA algorithm preserves the framework of CS-WOA from increasing its computational complexity, so that it remains the same order of complexity as $O(R{\cdot}m{\cdot}t_{max})$. In our work, the parameters of m, g and d are defined as a constant equaling to the number of pilot symbols P. Consequently, it makes the computational complexity on the same order of magnitude when the same population size R and iteration number t_{max} are applied for each algorithm.

From the result analysis, it reveals that, although the four intelligent algorithms have almost the same order of computational complexity, the proposed CS-EWOA algorithm outperforms CS-GA, CS-PSO, and CS-WOA by providing superior performance on BER, MSE, and convergence for pilot allocation optimization.

V. CONCLUSIONS

In this paper, an enhanced WOA algorithm, EWOA, is proposed based on four optimization strategies to effectively balance the exploitation and exploration. Subsequently, EWOA is associated with the CS theory, termed as CS-EWOA, to handle the optimization problem of pilot allocation for channel estimation in UWA-OFDM systems. According to the simulation results, the improvement of EWOA is verified with the best global solutions for the majority of testing on classical benchmark functions over other well-known metaheuristic algorithms. Our proposed CS-EWOA algorithm outperforms the equispaced, random, GA, PSO, and WOA based pilot allocation methods with both superior BER and MSE performance. Meanwhile, the robustness of CS-EWOA is demonstrated through the simulations by maintaining the consistent performance advantage over other considered methods for various situations and conditions, such as different types of channel models and varying subcarrier numbers in UWA-OFDM systems. Moreover, the convergence performance and computational complexity of CS-EWOA are

compared with CS-GA, CS-PSO, and CS-WOA in the iteration process of pilot allocation optimization. CS-EWOA keeps almost the same order of computational complexity with others, however, it yields strong performance on searching the optimal solution with higher convergence accuracy and faster convergence speed due to the outstanding tradeoff ability of exploitation and exploration. Additionally, since optimizing pilot allocation is accomplished in the design stage of UWA-OFDM systems, CS-EWOA does not sacrifice the real-time performance or introduce extra consumption. From these analyses, it can be concluded that our proposed CS-EWOA algorithm is a promising approach to optimize pilot allocation for channel estimation with superior performance of BER, MSE, and convergence in UWA-OFDM systems. The ensuing work will focus on employing the proposed CS-EWOA algorithm and its multi-objective variant to address the optimization problem of associative pilot symbol values and pilot allocation positions.

REFERENCES

[1] J. Huang, J. Sun, C. He, X. Shen, and Q. Zhang, "High-speed underwater acoustic communication based on OFDM," in *Proc. IEEE Int. Symp. Microw., Antenna, Propag. EMC Technol. Wireless Commun.*, vol. 2, Aug. 2005, pp. 1135–1138.

[2] X. Huang and V. B. Lawrence, "Bandwidth-efficient bit and power loading for underwater acoustic OFDM communication system with limited feedback," in *Proc. IEEE 73rd Veh. Technol. Conf.*, Yokohama, Japan, May 2011, pp. 1–5.

[3] A. Radosevic, T. M. Duman, J. G. Proakis, and M. Stojanovic, "Selective decision directed channel estimation for UWA OFDM systems," in *Proc. 49th Annu. Allerton Conf. Commun., Control, Comput.*, Monticello, IL, USA, Sep. 2011, pp. 647–653.

[4] A. B. Singh and V. K. Gupta, "Performance evaluation of MMSE and LS channel estimation in OFDM system," *Int. J. Eng. Trends Technol.*, vol. 15, no. 1, pp. 39–43, 2014.

[5] D. L. Donoho, "Compressed sensing," *IEEE Trans. Inf. Theory*, vol. 52, no. 4, pp. 1289–1306, Apr. 2006.

[6] G. Taubock and F. Hlawatsch, "A compressed sensing technique for OFDM channel estimation in mobile environments: Exploiting channel sparsity for reducing pilots," in *Proc. IEEE Int. Conf. Acoust., Speech Signal Process.*, Las Vegas, NV, USA, Mar. 2008, pp. 2885–2888.

[7] C. R. Berger, S. Zhou, J. C. Preisig, and P. Willett, "Sparse channel estimation for multicarrier underwater acoustic communication: From subspace methods to compressed sensing," *IEEE Trans. Signal Process.*, vol. 58, no. 3, pp. 1708–1721, Mar. 2010.

[8] C. R. Berger, Z. Wang, J. Huang, and S. Zhou, "Application of compressive sensing to sparse channel estimation," *IEEE Commun. Mag.*, vol. 48, no. 11, pp. 164–174, Nov. 2010.

[9] L. Tang, H. Wu, R. Jiang, and C. Lu, "An improved pilot routing algorithm for compressed sensing-based channel estimation in underwater acoustic OFDM system," in *Proc. 9th Int. Conf. Adv. Infocomm Technol. (ICAIT)*, Chengdu, China, Nov. 2017, pp. 90–94.

[10] R. Jiang, S. Cao, W. Gao, and X. Wang, "Grey correlation degree analysis on pilot pattern optimization for OFDM channel estimation," in *Proc. IEEE Global Commun. Conf. (GLOBECOM)*, Dec. 2018, pp. 1–6.

[11] J. A. Tropp, "Greed is good: Algorithmic results for sparse approximation," *IEEE Trans. Inf. Theory*, vol. 50, no. 10, pp. 2231–2242, Oct. 2004.

[12] X. He, R. Song, and W. P. Zhu, "Optimal pilot pattern design for compressed sensing-based sparse channel estimation in OFDM systems," *Circuits Syst. Signal Process.*, vol. 31, no. 4, pp. 1379–1395, Aug. 2012.

[13] C. Qi and L. Wu, "A study of deterministic pilot allocation for sparse channel estimation in OFDM systems," *IEEE Commun. Lett.*, vol. 16, no. 5, pp. 742–744, May 2012.

[14] C. Qi, G. Yue, L. Wu, and A. Nallanathan, "Pilot design for sparse channel estimation in OFDM-based cognitive radio systems," *IEEE Trans. Veh. Technol.*, vol. 63, no. 2, pp. 982–987, Feb. 2014.

[15] C. Qi, G. Yue, L. Wu, Y. Huang, and A. Nallanathan, "Pilot design schemes for sparse channel estimation in OFDM systems," *IEEE Trans. Veh. Technol.*, vol. 64, no. 4, pp. 1493–1505, Apr. 2015.

[16] J. H. Holland, "Genetic algorithms," *Sci. Amer.*, vol. 267, no. 1, pp. 66–73, 1992.

[17] J. Kennedy and R. Eberhart, "Particle swarm optimization," in *Proc. IEEE Int. Conf. Neural Netw.*, Nov. 1995, pp. 1942–1948.

[18] D. Karaboga and B. Basturk, "A powerful and efficient algorithm for numerical function optimization: Artificial bee colony (ABC) algorithm," *J. Global Optim.*, vol. 39, no. 3, pp. 459–471, Apr. 2007.

[19] X.-S. Yang, "A new metaheuristic bat-inspired algorithm," *Nature Inspired Cooperat. Strategies Optim.*, vol. 284, pp. 65–74, 2010. [Online]. Available: https://link.springer.com/chapter/10.1007/978-3-642-12538-6_6

[20] S. Mirjalili, S. M. Mirjalili, and A. Lewis, "Grey wolf optimizer," *Adv. Eng. Softw.*, vol. 69, pp. 46–61, Mar. 2014.

[21] S. Mirjalili and A. Lewis, "The whale optimization algorithm," *Adv. Eng. Softw.*, vol. 95, pp. 51–67, May 2016.

[22] I. Aljarah, H. Faris, and S. Mirjalili, "Optimizing connection weights in neural networks using the whale optimization algorithm," *Soft Comput.*, vol. 22, no. 1, pp. 1–15, 2016.

[23] A. H. Gandomi, X.-S. Yang, A. H. Alavi, and S. Talatahari, "Bat algorithm for constrained optimization tasks," *Neural Comput Appl.*, vol. 22, no. 6, pp. 1239–1255, 2013.

[24] S. Arora and S. Singh, "Node localization in wireless sensor networks using butterfly optimization algorithm," *Arabian J. Sci. Eng.*, vol. 42, no. 8, pp. 3325–3335, Aug. 2017.

[25] M. N. Seyman and N. Taşpinar, "Particle swarm optimization for pilot tones design in MIMO-OFDM systems," *EURASIP J. Adv. Signal Process.*, vol. 2011, no. 1, pp. 1–11, 2011.

[26] X. He, R. Song, and W.-P. Zhu, "Pilot allocation for distributed-compressed-sensing-based sparse channel estimation in MIMO-OFDM systems," *IEEE Trans. Veh. Technol.*, vol. 65, no. 5, pp. 2990–3004, May 2016.

[27] L. Najjar, "Pilot allocation by genetic algorithms for sparse channel estimation in OFDM systems," in *Proc. 21st Eur. Signal Process. Conf.*, Marrakesh, Morocco, Sep. 2013, pp. 1–5.

[28] N. Taşpinar and C. S. Şimşir, "Pilot tones design using particle swarm optimization for OFDM–IDMA system," *Neural Comput. Appl.*, vol. 1, pp. 1–10, Feb. 2018.

[29] M. N. Seyman and N. Taşpınar, "Pilot tones optimization using artificial bee colony algorithm for MIMO–OFDM systems," *Wireless Pers. Commun.*, vol. 71, no. 1, pp. 151–163, Jul. 2013.

[30] C. S. Şimşir and N. Taşpınar, "Pilot tones design using grey wolf optimizer for OFDM–IDMA system," *Phys. Commun.*, vol. 25, pp. 259–267, Dec. 2017.

[31] N. Taşpinar and C. S. Şimşir, "An efficient technique based on firefly algorithm for pilot design process in OFDM–IDMA systems," *Turkish J. Electr. Eng. Comput. Sci.*, vol. 26, no. 2, pp. 817–829, Mar. 2018.

[32] C. Knievel and P. A. Hoeher, "On particle swarm optimization for MIMO channel estimation," *J. Electr. Comput. Eng.*, vol. 1, no. 6, pp. 1–10, Jan. 2012.

[33] Y. Nie, X. Yu, and Z. Yang, "Deterministic pilot pattern allocation optimization for sparse channel estimation based on CS theory in OFDM system," *EURASIP J. Wireless Commun. Netw.*, vol. 7, no. 1, pp. 1–8, Dec. 2019.

[34] K. Vidhya and K. R. S. Kumar, "Channel estimation of MIMO–OFDM system using PSO and GA," *Arabian J. Sci. Eng.*, vol. 39, no. 5, pp. 4047–4056, May 2014.

[35] J. Sujitha and K. Baskaran, "Genetic grey wolf optimizer based channel estimation in wireless communication system," *Wireless Pers. Commun.*, vol. 99, no. 2, pp. 965–984, Mar. 2018.

[36] W. A. Watkins and W. E. Schevill, "Aerial observation of feeding behavior in four baleen whales: Eubalaena glacialis, Balaenoptera borealis, megaptera novaeangliae, and Balaenoptera physalus," *J. Mammal.*, vol. 60, no. 1, pp. 155–163, Feb. 1979.

[37] D. Oliva, M. A. El Aziz, and A. E. Hassanien, "Parameter estimation of photovoltaic cells using an improved chaotic whale optimization algorithm," *Appl. Energy*, vol. 200, pp. 141–154, Aug. 2017.

[38] G. Xiong, J. Zhang, D. Shi, and Y. He, "Parameter extraction of solar photovoltaic models using an improved whale optimization algorithm," *Energy Convers. Manage.*, vol. 174, pp. 388–405, Oct. 2018.

[39] D. Prasad, A. Mukherjee, G. Shankar, and V. Mukherjee, "Application of chaotic whale optimisation algorithm for transient stability constrained optimal power flow," *IET Sci. Meas. Technol.*, vol. 11, no. 8, pp. 1002–1013, Nov. 2017.

[40] W. Z. Sun and J. S. Wang, "Elman neural network soft-sensor model of conversion velocity in polymerization process optimized by chaos whale optimization algorithm," *IEEE Access*, vol. 5, pp. 13062–13076, 2017.

[41] Y. Ling, Y. Zhou, and Q. Luo, "Lévy flight trajectory-based whale optimization algorithm for global optimization," *IEEE Access*, vol. 5, pp. 6168–6186, 2017.

[42] Y. Zheng, Y. Li, G. Wang, Y. Chen, Q. Xu, J. Fan, and X. Cui, "A novel hybrid algorithm for feature selection based on whale optimization algorithm," *IEEE Access*, vol. 7, pp. 14908–14923, 2018.

[43] J. Luo and B. Shi, "A hybrid whale optimization algorithm based on modified differential evolution for global optimization problems," *Appl. Intell.*, vol. 49, no. 5, pp. 1982–2000, May 2019.

[44] A. A. Ewees, M. A. Elaziz, and D. Oliva, "Image segmentation via multilevel thresholding using hybrid optimization algorithms," *J. Electron. Imag.*, vol. 27, no. 6, 2018, Art. no. 063008.

[45] P. Chen, Y. Rong, S. Nordholm, Z. He, and A. J. Duncan, "Joint channel estimation and impulsive noise mitigation in underwater acoustic OFDM communication systems," *IEEE Trans. Wireless Commun.*, vol. 16, no. 9, pp. 6165–6178, Sep. 2017.

[46] C. Qi, X. Wang, and L. Wu, "Underwater acoustic channel estimation based on sparse recovery algorithms," *IET Signal Process.*, vol. 5, no. 8, pp. 739–747, 2011.

[47] E. Panayirci, M. T. Altabbaa, M. Uysal, and H. V. Poor, "Sparse channel estimation for OFDM-based underwater acoustic systems in Rician fading with a new OMP-MAP algorithm," *IEEE Trans. Signal Process.*, vol. 67, no. 6, pp. 1550–1565, Mar. 2019.

[48] B. Li, S. Zhou, M. Stojanovic, L. Freitag, and P. Willett, "Multicarrier communication over underwater acoustic channels with nonuniform Doppler shifts," *IEEE J. Ocean. Eng.*, vol. 33, no. 2, pp. 198–209, Apr. 2008.

[49] M. T. Altabbaa and E. Panayirci, "Channel estimation and equalization algorithm for OFDM-based underwater acoustic communications systems," in *Proc. 13th Int. Conf. Wireless Mobile Commun. (ICWMC)*, Nice, France, Jul. 2017, pp. 113–118.

[50] M. T. Altabbaa, A. S. Ogrenci, E. Panayirci, and H. V. Poor, "Sparse channel estimation for space-time block coded OFDM-based underwater acoustic channels," in *Proc. IEEE Global Commun. Conf. (GLOBECOM)*, Dec. 2018, pp. 1–6.

[51] J. A. Tropp and A. C. Gilbert, "Signal recovery from random measurements via orthogonal matching pursuit," *IEEE Trans. Inf. Theory*, vol. 53, no. 12, pp. 4655–4666, Dec. 2007.

[52] D. Needell and J. A. Tropp, "CoSaMP: Iterative signal recovery from incomplete and inaccurate samples," *Appl. Comput. Harmon. Anal.*, vol. 26, no. 3, pp. 301–321, 2009.

[53] E. J. Candés, J. K. Romberg, and T. Tao, "Stable signal recovery from incomplete and inaccurate measurements," *Commun. Pure Appl. Math.*, vol. 59, no. 8, pp. 1207–1223, 2006.

[54] D. L. Donoho, M. Elad, and V. N. Temlyakov, "Stable recovery of sparse overcomplete representations in the presence of noise," *IEEE Trans. Inf. Theory*, vol. 52, no. 1, pp. 6–18, Jan. 2006.

[55] V. Abolghasemi, S. Ferdowsi, B. Makkiabadi, and S. Sanei, "On optimization of the measurement matrix for compressive sensing," in *Proc. Eur. Signal Process. Conf.*, Aalborg, Denmark, Aug. 2010, pp. 427–431.

[56] C. Lu, H. Li, and Z. Lin, "Optimized projections for compressed sensing via direct mutual coherence minimization," *Signal Process.*, vol. 151, pp. 45–55, Oct. 2018.

[57] D. L. Donoho and P. B. Stark, "Uncertainty principles and signal recovery," *SIAM J. Appl. Math.*, vol. 49, no. 3, pp. 906–931, Jun. 1989.

[58] Y. Liu and S. Li, "Hybrid good point set evolutionary strategy for constrained optimization," *Commun. Comput. Inf. Sci.*, vol. 93, pp. 30–39, Aug. 2010.

[59] R. Y. Jia, Z. H. Jia, and J. W. Geng, "Case-based reasoning based on good-point-set genetic algorithm and its application," *Adv. Mater. Res.*, vol. 217, pp. 886–892, Jan. 2011.

[60] X. Liu, S. B. Xuan, and F. Liu, "An advanced particle swarm optimization based on good-point set and application to motion estimation," in *Proc. Int. Conf. Intell. Comput. Theories Technol.*, Nanning, China, Jul. 2013, pp. 494–502.

[61] G. Kaur and S. Arora, "Chaotic whale optimization algorithm," *J. Comput. Des. Eng.*, vol. 5, no. 3, pp. 275–284, 2018.

[62] D. Yousri, D. Allam, and M. B. Eteiba, "Chaotic whale optimizer variants for parameters estimation of the chaotic behavior in permanent magnet synchronous motor," *Appl. Soft Comput.*, vol. 74, pp. 479–503, Jan. 2019.

[63] N. Khashan, M. A. Elhosseini, A. Y. Haikal, and M. Badawy, "Biped robot stability based on an A–C parametric whale optimization algorithm," *J. Comput. Sci.*, vol. 31, pp. 17–32, Feb. 2018.

[64] Y. Sun, X. Wang, Y. Chen, and Z. Liu, "A modified whale optimization algorithm for large-scale global optimization problems," *Expert Syst. Appl.*, vol. 114, pp. 563–577, Dec. 2018.

[65] B. Karlik and A. Vehbi, "Performance analysis of various activation functions in generalized MLP architectures of neural networks," *Int. J. Artif. Intell. Expert Syst.*, vol. 1, no. 4, pp. 111–122, 2015.

[66] R. Jiang, X. Wang, S. Cao, J. Zhao, and X. Li, "Deep neural networks for channel estimation in underwater acoustic OFDM systems," *IEEE Access*, vol. 7, pp. 23579–23594, 2019.

[67] S. Mahdavi, S. Rahnamayan, and K. Deb, "Opposition based learning: A literature review," *Swarm Evol. Comput.*, vol. 39, pp. 1–23, Apr. 2018.

[68] S. Rahnamayan, H. R. Tizhoosh, and M. M. A. Salama, "Opposition versus randomness in soft computing techniques," *Appl. Soft Comput.*, vol. 8, no. 2, pp. 906–918, Mar. 2008.

[69] S. Mirjalili, "Moth-flame optimization algorithm: A novel nature-inspired heuristic paradigm," *Knowl.-Based Syst.*, vol. 89, pp. 228–249, Nov. 2015.

[70] S. Mirjalili and S. Z. M. Hashim, "A new hybrid PSOGSA algorithm for function optimization," in *Proc. Int. Conf. Comput. Inf. Appl.*, Tianjin, China, Dec. 2010, pp. 374–377.

[71] M. B. Porter, "The BELLHOP manual and user's guide: Preliminary draft," Heat, Light, and Sound Research, Inc., La Jolla, CA, USA, Tech. Rep., 2011. [Online]. Available: http://oalib.hlsresearch.com/Rays/HLS-2010-1.pdf

[72] R. Jiang, S. Cao, C. Xue, and L. Tang, "Modeling and analyzing of underwater acoustic channels with curvilinear boundaries in shallow ocean," in *Proc. IEEE Int. Conf. Signal Process., Commun. Comput. (ICSPCC)*, Oct. 2017, pp. 1–6.

[73] X. Wang, X. Wang, R. Jiang, W. Wang, Q. Chen, and X. Wang, "Channel modelling and estimation for shallow underwater acoustic OFDM communication via simulation platform," *Appl. Sci.*, vol. 9, no. 3, p. 447, Jan. 2019.

[74] (2018). *Aviso Satellite Altimetry Data*. [Online]. Available: http://www.aviso.altimetry.fr

[75] (2014). *Google Maps Platform*. [Online]. Available: https://cloud.google.com/maps-platform/

[76] A. M. T. Boyer. (2014). *World Ocean Atlas 2013 Product Documentation*. [Online]. Available: http://www.nodc.noaa.gov/OC5/indprod.html

[77] C. Bjerrum-Niese and R. Lutzen, "Stochastic simulation of acoustic communication in turbulent shallow water," *IEEE J. Ocean. Eng.*, vol. 25, no. 4, pp. 523–532, Oct. 2000.

[78] S. Zhou and Z. Wang, *OFDM for Underwater Acoustic Communications*. Hoboken, NJ, USA: Wiley, 2014.

[79] D. Truhachev, C. Schlegel, M. Bashir, and J.-F. Bousquet, "Modeling of underwater acoustic channels for communication system testing," in *Proc. MTS/IEEE Charleston*, Charleston, SC, USA, Oct. 2018, pp. 1–8.

[80] R. G. Baraniuk, "Compressive sensing," *IEEE Signal Process. Mag.*, vol. 24, no. 4, pp. 118–121, Jul. 2007.

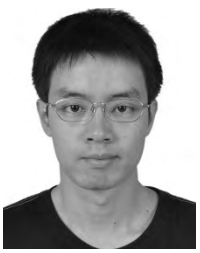

RONGKUN JIANG received the B.Eng. degree in electronic information engineering from the School of Information and Electronics, Beijing Institute of Technology, Beijing, China, in 2012, where he is currently pursuing the Ph.D. degree in electronic science and technology engineering. His research interests include underwater acoustic communication, OFDM systems, compressed sensing, channel estimation with applications of neural networks, and swarm intelligence algorithms.

XUETIAN WANG received the B.Eng. and Ph.D. degrees in electronic engineering from the Beijing Institute of Technology, Beijing, China, in 1986 and 2002, respectively, where he is currently a Full Professor with the School of Information and Electronics. His current research interests include antenna theory and applications, millimeter-wave imaging, EMC, and terahertz radar.

SHAN CAO received the B.Eng. and Ph.D. degrees in microelectronics from Tsinghua University, China, in 2009 and 2015, respectively. She is currently an Assistant Professor with Shanghai University, China. Her research interests include design and implementation of wireless communication systems, design and implementation of signal processing systems, and integrated circuit design of neural networks.

JIAFEI ZHAO received the B.Eng. degree from the Chongqing University of Posts and Telecommunications, Chongqing, China, in 2013. She is currently pursuing the Ph.D. degree in electronic science and technology engineering with the School of Information and Electronics, Beijing Institute of Technology, Beijing. Her current research interests include clutter generation, system modeling, and neural networks.

XIAORAN LI received the B.Eng. degree in telecommunication engineering from the Beijing University of Posts and Telecommunications, Beijing, China, in 2011, and the M.E. and Ph.D. degrees in electronics science and technology from the Beijing Institute of Technology, Beijing, in 2013 and 2017, respectively. She was a Visiting Scholar with the Department of Electrical and Computer, Duke University, NC, USA, from 2015 to 2016. She is currently a Postdoctoral Research Fellow with the School of Information and Electronics, Beijing Institute of Technology. Her research interests include analog, radio frequency (RF) and millimeter-wave (MMW) integrated circuits design, and circuits for biomedical applications.